Microemulsion-based interfacial diffusion synthesis of uniform BaCO$_3$ nanorods

Xianda He[a], Jinye Ran, Wenyu Zhang and Hongchuan Fu

School of Chemistry and Chemical Engineering, Southwest University, Chongqing 400715, PR China

[a]davidhe4@swu.edu.cn

Keywords: Interfaces; Diffusion; Synthesis; Barium carbonate; Nanorods; Nanoparticles.

Abstract. Uniform BaCO$_3$ nanorods were successfully synthesized by a novel microemulsion-based interfacial diffusion method using a lipophilic organic carbonate $(CH_3CH_2)_2CO_3$ as the precipitating agent. For comparison, two other similar methods, namely interfacial diffusion method in the absence of microemulsion and the traditional two-microemulsion method, were also investigated. In contrast, only micron-sized needles and irregular nanoparticles were generated via the latter two methods. We suggest a diffusion-controlled interfacial nucleation followed by oriented growth mechanism coupled with the confinement effect of microemulsion droplets to explain the formation of uniform nanorods. Selected-area electron diffraction (SAED) patterns indicated that BaCO$_3$ samples produced by the three similar methods were in distinct crystalline states.

Introduction

Barium carbonate (BaCO$_3$) has attracted a lot of research interest due to its importance both as a common natural mineral and as an industrial chemical widely used in brick, glass, ceramics, oil-drilling, and photographic industries [1]. Submicron-sized and nanosized powders and structures with specific shape normally show interesting properties and considerable potential applications. Thus, size- and shape-controlled synthesis of BaCO$_3$ has become the focus of research attention [2]. To manipulate nucleation and growth of the solid product formation process, which is critical for size and shape control of BaCO$_3$, a great many techniques have been investigated during the past decade.

Ultrasonic irradiation [3] and microwave heating [4] have been adopted to intensifying reaction conditions for fast nucleation resulting in irregular BaCO$_3$ aggregates. On the other hand, hydrothermal method has been employed for organized growth of BaCO$_3$ crystals [5]. Organic growth modifiers have also been used for creating various BaCO$_3$ superstructures and nanostructures [6-8]. Besides, the addition of a surfactant along with the organic solvent into the aqueous solution would result in a w/o microemulsion, in which the thermodynamically stable surfactant-encapsulated water droplets are taken as excellent microreactors for preparing nanomaterials. BaCO$_3$ nanowires synthesized in microemulsion systems has been reported [9].

Despite all the efforts attempted, the generation of highly uniform nanosized BaCO$_3$ remains a challenging task to the synthetic chemists. In this paper, we propose to introduce a lipophilic organic carbonate for release of CO_3^{2-} migrating through the surfactant layer into the Ba^{2+}-containing water droplets in the microemulsion dispersion. We demonstrate that uniform BaCO$_3$ nanorods can thus be obtained. For comparison, two other similar methods are also investigated.

Experiment

Barium hydroxide (aqueous) and carbonate (aqueous or cyclohexane) solutions were used as reactants. As illustrated in Fig. 1, BaCO$_3$ were synthesized via three methods: (A) interfacial diffusion method, (B) two-microemulsion method, and (C) one-microemulsion interfacial diffusion method. All the experiments were carried out at room temperature.
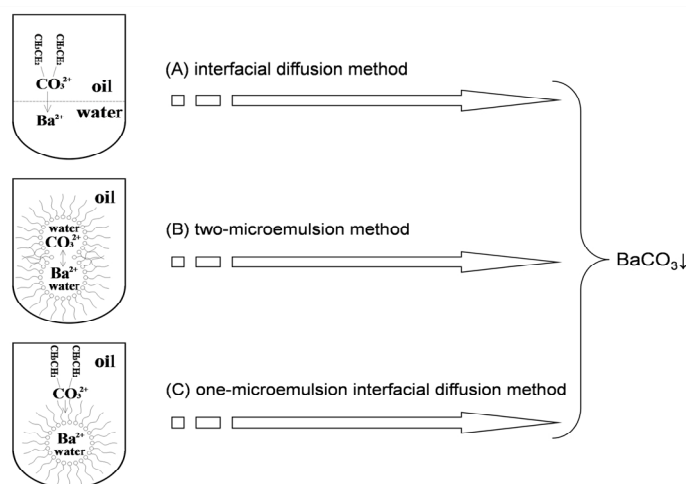
Fig. 1. Schematic illustration of the three methods for synthesis of $BaCO_3$

In method A, 0.4 ml of $Ba(OH)_2$ solution (0.1 M aqueous) and 0.4 ml of $(CH_3CH_2)_2CO_3$ solution (0.5 M cyclohexane) were added with shaking to 10 ml of cyclohexane successively. In method B, two types of w/o microemulsions were prepared separately. Both microemulsions were stabilized by the nonionic surfactant nonylphenol polyoxyethylene (6) ether (NP-6). The first microemulsion was prepared in the composition of 2 g NP-6/10 ml cyclohexane/0.4 ml $Ba(OH)_2$ solution (0.1 M aqueous). The second microemulsion was prepared in the composition of 2 g NP-6/10 ml cyclohexane/0.4 ml Na_2CO_3 solution (0.1 M aqueous). The nanosized $BaCO_3$ was obtained by addition with shaking of the second microemulsion to the first one. In method C, a microemulsion was first prepared by the mixing of 0.4 ml of aqueous $Ba(OH)_2$ (0.1 M) and 1 g or 2 g of NP-6 in 10 ml of cyclohexane. 0.4 ml of $(CH_3CH_2)_2CO_3$ solution (0.5 M cyclohexane) was then added with shaking to the as-prepared microemulsion.

For all three methods, the mixed solutions were kept still in a test tube for 3 hours before solid-liquid separation by a centrifuge at 6000 rpm for 15 minutes. Appropriate amount of absolute ethanol and deionized water were added to the solid-liquid mixture before the centrifugal separation. The washing and centrifuging operation was conducted for at least six times. The final $BaCO_3$ products were dried in an oven at 60 ℃ overnight and collected for further characterization.

The $BaCO_3$ samples were identified by Fourier transform infrared (FTIR) spectroscopy on a Bruker TENSOR 27 spectrometer. The size and shape of the synthesized $BaCO_3$ were observed by using a JEOL JEM-6700F field-emission scanning electron microscope (SEM) operating at 10 kV. Transmission electron microscope (TEM) imaging and selected-area electron diffraction (SAED) were carried out on a JEOL JEM-2100 instrument with accelerating voltage of 200 kV.

Results and Discussion

The corresponding IR spectra of three samples via method A, B and C are shown in Fig. 2. All the spectra exhibited absorption peaks at 1751, 1451, 1059, 857 and 693 cm^{-1}, which represent the characteristic absorbance of $BaCO_3$ with high purity [7]. The isolated planar CO_3^{2-} anion has a D3h symmetry. The absorption bands attributed to the vibrations in CO_3^{2-} anion are located within the 1800-400 cm^{-1} region. From the IR spectra one can observe a strong broad absorption band centered about 1451 cm^{-1} and a weak absorption band at 1059 cm^{-1} due to the asymmetric and symmetric C-O stretching vibration respectively. And the sharp absorption bands at about 857 cm^{-1} and 693 cm^{-1} can be assigned to the out-of-plane bending and in-plane bending modes of CO_3^{2-}, respectively. The O-H bending vibrations of residual water contained in $BaCO_3$ were also detected at 1647 cm^{-1} [4]. In addition, the absorption peak of 1751 cm^{-1} could be attributed to the combination of symmetric stretching vibrations and in-plane vibrations.
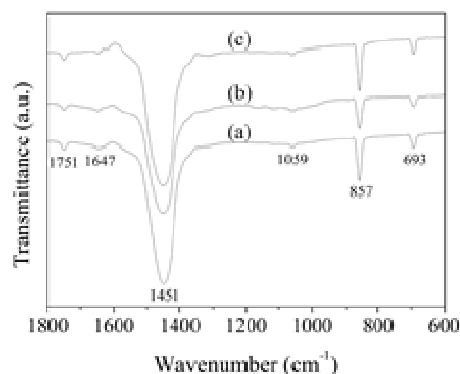
Fig. 2. IR spectra of $BaCO_3$ synthesized by different methods: (a) method A; (b) method B; (c) method C.
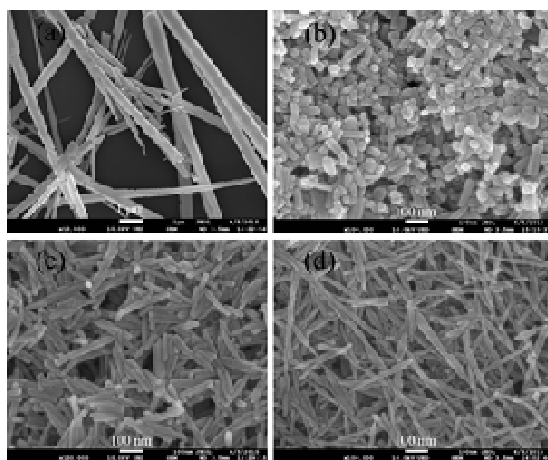

Fig. 3. SEM images of $BaCO_3$ synthesized by different methods: (a) method A; (b) method B; (c) and (d) method C with 1 g and 2 g of NP-6 respectively.
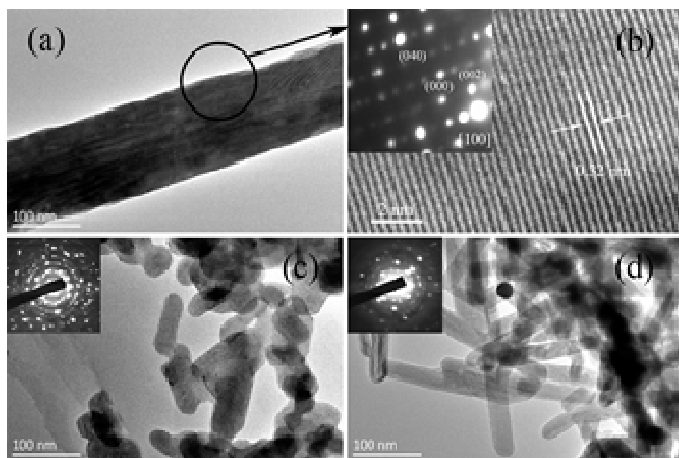

Fig. 4. TEM and SAED images of $BaCO_3$ synthesized by different methods: (a) and (b) method A; (c) method B; (d) method C.

Fig. 3 shows the SEM images of typical products prepared by the three methods. It can be seen in Fig. 3a that $BaCO_3$ needles with a size up to the micron range were produced via method A in the absence of surfactant NP-6. In contrast, nanosized products as indicated in Fig. 3b, 3c and 3d were generated via the microemulsion-based method B and C, which can be considered as the result of confinement effect of the microemulsion droplets. Fig. 3a show that unevenly distributed $BaCO_3$ averaged about 40 nm in size composed of nanospheroids, nanorods and nanoaggregates were synthesized by method B. Fig. 3c and 3d show the rather uniform and separated nanorods about 25 nm

in diameter prepared by method C. By comparison, with a higher surfactant content nanorods of higher length/diameter ratio and lower diameter were observed in Fig. 3d than in Fig. 3c.

Typical TEM and SAED images of the $BaCO_3$ samples are shown in Fig. 4. The SAED pattern in Fig. 4b indicates the single-crystalline nature of the needle-shaped product (Fig. 4a) produced via method A in the absence of surfactant. The SAED diffraction spots were observed due to the [100] zone axis of the witherite phase (JCPDS 05-0378), which is quite frequently reported in the literature [2-5]. High-resolution TEM image in Fig. 4b exhibited a periodic fringe space of 0.32 nm, which corresponds to the lattice spacing of (002) planes. Considering the SAED pattern and TEM image together, it is reasonable to conclude that the $BaCO_3$ needles grew preferentially in the [002] direction. Fig. 4c presents the TEM image of the irregular nanoparticles via method B. The corresponding circular SEAD pattern in Fig. 4c exhibited a polycrystalline feature. Fig. 4d shows the TEM image of the uniform and highly separated nanorods via method C. It is interesting that the corresponding SEAD pattern seems to be in periodic order to some extent. The distinction in morphology and crystalline state between the samples can be accounted for by assuming an engulfment-induced burst nucleation followed by aggregative growth mechanism for method B and a diffusion-controlled interfacial nucleation followed by oriented growth mechanism for method A and C.

Conclusions

In summary, we have developed a novel microemulsion-based interfacial diffusion method with lipophilic organic carbonate as precipitant to obtain rather uniform $BaCO_3$ nanorods about 25 nm in diameter. By contrast, only micron-sized needles and irregular nanoparticles were generated via interfacial diffusion method in the absence of microemulsion and the traditional two-microemulsion method respectively. A diffusion-controlled interfacial nucleation followed by oriented growth mechanism and the confinement effect of microemulsion droplets could explain the formation of uniform nanorods obtained via the novel method. Based on such assumptions, we suggest the introduction of other lipophilic precipitating agent into the microemulsion continuous phase for interfacial diffusion synthesis of various highly uniform inorganic nanomaterials.

Acknowledgments

Literature References

[1] R.C. Ropp: *Encyclopedia of the Alkaline Earth Compounds* (Elsevier, Amsterdam 2013).

[2] X. Ma, C. Su, L. Yang, L. Li, K. Wang, J. Zhou and S. Yuan: CrystEngComm Vol. 14 (2012), p. 8554.

[3] M.A. Alavi and A. Morsali: Ultrason. Sonochem. Vol. 15 (2008), p. 833.

[4] N. Tipcompor, T. Thongtem, A. Phuruangrat and S. Thongtem: Mater. Lett. Vol. 87 (2012), p. 153.

[5] J. Xu and D. Xue: J. Phys. Chem. Solids Vol. 67 (2006), p. 1427.

[6] Y. Ni, X. Li, J. Hong and X. Ma: Mater. Chem.Phys. Vol. 120 (2010), p. 10.

[7] S. Lv, P. Li, J. Sheng and W. Sun: Mater. Lett. Vol. 61 (2007), p. 4250.

[8] Y. Zhang, B. Xie and R. Zhang: New J. Chem. (2018), in press.

[9] L. Qi, J. Ma, H. Cheng and Z. Zhao: J. Phys. Chem. B Vol. 101 (1997), p. 3460.